

A Comparison of new MC-adapted Parton Densities

T. Kasemets* and T. Sjöstrand†

*Theoretical High Energy Physics
Department of Astronomy and Theoretical Physics,
Lund University,
Sölvegatan 14A,
SE 223 62 Lund, Sweden*

Abstract

A selection of the latest and most frequently used parton distribution functions (PDFs) is incorporated in PYTHIA8, including the Monte Carlo-adapted PDFs from the MSTW and CTEQ collaborations. This article examines the differences in PDFs as well as the effect they have on results of simulations and compare with data collected by the CDF experiment. Monte Carlo-adapted PDFs do a better job than leading- and next-to-leading order PDFs for many observables, but there is room for further improvements.

1 Introduction

Precision measurements of cross sections should be compared with precision theoretical calculations. The state of the art is next-to-leading order (NLO) calculations of matrix elements (MEs), which then should be combined with NLO parton distribution functions (PDFs) to obtain the theoretical predictions for various processes at hadron colliders. Such an approach works well for sufficiently inclusive quantities, say the total cross section for W^\pm production.

At the other extreme, say for the production of jets associated with the W^\pm , experimental jet finding will be based on the clustering of a complex hadronic final state. Currently such states

can only be modeled by the use of event generators, where many components are only formulated to leading order (LO), such as multiparton interactions (MPIs), initial-state radiation (ISR) and final-state radiation (FSR). In these descriptions it is thus not appropriate to use NLO PDFs.

To be more specific, the combination of LO MEs with NLO PDFs is accurate to LO, just as LO MEs with LO PDFs would be. So from a formal point of view the use of NLO or LO PDFs is equivalent. There is a key point, however: LO PDFs have a simple probabilistic interpretation and are always positive, as are LO MEs. At NLO positivity is no longer required, neither for PDFs nor for MEs. The convolution of the two hopefully should still be positive, but even that is strictly not guaranteed over all of phase space. Characteristic for NLO PDFs is especially that the gluon distribution at small x

*tomas@kasemets.se

†torbjorn@thep.lu.se

and Q^2 tends to come out negative, or at least very small, in order to describe the evolution of F_2 with Q^2 . This means that the LO ME + NLO PDF combination breaks down in this region, which is where most of the underlying-event activity originates (from MPIs, ISR and FSR).

Thus there is a need to continue the development and use of LO PDFs. In recent years this field has received renewed attention [1]-[3]. In particular, attempts have been made to find LO PDFs that, when combined with LO MEs, attach better to the complete NLO behavior for a selection of cross sections. This is accomplished primarily by relaxing the momentum sum rule, in order to allow the PDFs to have a large small- x gluon distribution without compromising the large- x quark distributions. Studying these new PDFs can shed more light on which features of the PDFs are ideal for leading-order MC generators and how further improvements can be made.

To this end we have incorporated ten new PDFs into PYTHIA8 [4] and compare the new MC-adapted PDFs with regular LO and NLO PDFs. We also study how the differences between them affect results of simulations, and compare the results with data collected by the CDF experiment. The observables studied are somewhat different from the ones used in the construction of the PDFs and thus give a complementary picture.

The structure of the article is as follows. Section 2 describes the inclusion of the PDFs in PYTHIA8. The different PDFs are compared in section 3. The results from simulations of minimum-bias events and hard QCD events are studied in sections 4 and 5, respectively. Finally the article concludes with a summary and outlook in section 6.

2 PDFs in PYTHIA8

PYTHIA8 has so far been distributed with the option to choose between two PDFs, GRV94L [5] and CTEQ5L [6], which are both fairly old. Many new and improved PDFs have been released and made available to PYTHIA8 simulations only through LHAPDF [7]. The LHAPDF package has grown quite large and in the process also somewhat slow, and the code is written in Fortran while the com-

munity is changing to C++. It is desirable to include some PDFs directly into PYTHIA8 since it can speed up simulations, make PYTHIA8 more complete and facilitate the switching between different frequently used PDFs. We therefore incorporate ten new PDFs from the MRST [1]-[2], MSTW 2008 [8], CTEQ6 [9] and CTEQ MC [3] distributions into PYTHIA8, listed in Tab. 1. Two of them are NLO, which are not intended for LO MC use, but included for comparison. Inclusion of the PDFs was done in close contact with the MSTW and CTEQ collaborations.

Including additional PDFs proved to be less straightforward than might first be expected, see further below. A major reason for this is the need to, in MC simulations, go outside the range of the PDF grids; specifically to smaller x and Q^2 values. MSTW provides routines not only for interpolation but also for extrapolation outside this grid, while the CTEQ collaboration has recommended a freeze of the PDFs at the value just inside the grid. The range of the grids for the different PDFs are shown in Tab. 1, together with their α_S values and running.

The code supplied by the authors had to be modified to fit natively into PYTHIA8 and we carried out extensive tests. When possible the tests included comparisons with the corresponding PDFs in the LHAPDF package. The PYTHIA8-included PDFs run about a factor two faster than they do going the way via the LHAPDF package.

2.1 MRST/MSTW

The PDFs supplied to us from MSTW were in some respects improved compared to the versions available in LHAPDF. Our implementation for the MRST LO* and LO** PDFs make use of the new MSTW grid (64×48) ranging down to $x = 10^{-6}$ while the LHAPDF versions use the original grid with fewer (49×37) grid points and shorter x range ($x_{min} = 10^{-5}$). The new grid results in a less steep gluon distribution towards small x , and at $x = 10^{-8}$ the difference reaches a factor of two. The values of α_S are slightly different in the new LO* and LO** grid files than in the corresponding LHAPDF ones. The LHAPDF versions use Λ_{QCD} for four active flavors, and the change to Λ_{QCD} for

PDF	x range	Q^2 range [GeV ²]	α_S	$\alpha_S(M_Z)$
GRV94L	$10^{-5} - 1$	$0.40 - 10^6$	LO	0.128
CTEQ5L	$10^{-6} - 1$	$1.00 - 10^8$	LO	0.127
MRST LO*	$10^{-6} - 1$	$1.00 - 10^9$	NLO	0.12032
MRST LO**	$10^{-6} - 1$	$1.00 - 10^9$	NLO	0.11517
MSTW LO	$10^{-6} - 1$	$1.00 - 10^9$	LO	0.13939
MSTW NLO	$10^{-6} - 1$	$1.00 - 10^9$	NLO	0.12018
CTEQ6L	$10^{-6} - 1$	$1.69 - 10^8$	NLO	0.1180
CTEQ6L1	$10^{-6} - 1$	$1.69 - 10^8$	LO	0.1298
CTEQ66 (NLO)	$10^{-8} - 1$	$1.69 - 10^{10}$	NLO	0.1180
CT09MC1	$10^{-8} - 1$	$1.69 - 10^{10}$	LO	0.1300
CT09MC2	$10^{-8} - 1$	$1.69 - 10^{10}$	NLO	0.1180
CT09MCS	$10^{-8} - 1$	$1.69 - 10^{10}$	NLO	0.1180

Table 1: The PDFs now included in PYTHIA8, with the x and Q^2 ranges of the respective grids, as well as the order of the running of α_S and the value at M_Z

five active flavors yields a slightly different value. Also worth noticing is that LO* and LO** both use the unorthodox value of the Z boson mass, $M_Z = 91.71$ GeV, unlike the MSTW 2008 distribution which uses $M_Z = 91.19$ GeV [7]. For MSTW 2008 LO, LO* and LO** the interpolation gave negative gluon values at some large- x intervals and for a wide range of Q^2 scales. The gluon distribution is very small in this region and therefore the negative values do not affect the results of the simulations. Furthermore, LHAPDF can give negative values for the up quark for $0.9 < x < 1.0$ at large Q^2 , which is worse since the up quark dominates for large x values.

The MSTW NLO distribution gave very large negative values for the anomalous dimension $\frac{d \log(xf)}{d \log(Q^2)}$ at small Q^2 and x values around 10^{-5} , which resulted in a huge \bar{s} distribution when extrapolated to low Q^2 . This could also be a problem for the gluon which could get large negative anomalous dimensions in the x region where the distribution is negative. To avoid this the anomalous dimension is manually forced to be larger than -2.5 . Although this does fix the issue at hand, it is also an example of the dangers of using NLO PDFs in LO MC simulations, and an indication that one has to be very careful with such use.

2.2 CTEQ 6/MC

The CTEQ distributions work well inside the grid but outside or near the edges some problems occurred. The $tv = \log(\log(Q))$ values in the grid file were discovered not to exactly correspond to the Q values in the same file, and hence some points inside the Q grid would end up outside the tv grid. This caused some strange errors, for example the b quark distribution, after being zero below the threshold, suddenly became huge at Q^2 values just inside the grid. Therefore we choose to read in only the Q grid points and then calculate tv .

Outside the grid there can be differences between the CTEQ6 PDFs in PYTHIA8 and the corresponding ones in LHAPDF. This is because LHAPDF provides the option to use extrapolation routines where PYTHIA8, by recommendation from the CTEQ authors, freezes the values.

3 Comparison of PDFs

There are strong similarities between the PDFs but also large differences, especially in the small x region. Broadly the LO PDFs are similar, except for MSTW LO which is much larger than the others for small x values, the MC-adapted PDFs are similar and the NLO PDFs are similar. Comparing the two groups, the CTEQ distributions have

smaller distributions at small x , both for the PDFs that freeze and for the ones with the grid ranging down to 10^{-8} , except for the NLO distributions. The two NLO PDFs have a smaller gluon distribution at small x , and MSTW NLO is negative at $Q^2 = 4 \text{ GeV}^2$.

The gluon distribution is dominating in the region of small x while the valence quarks, and then especially the up quarks, dominate for large x . For a first comparison we therefore choose to focus mainly on these two distributions.

The PDFs are different from one another in several aspects. Four of them do not obey the momentum sum rule. LO* carries 1.12 times the proton momentum, LO** a Q^2 -dependent number between 1.17 and 1.14, MC1 1.10 and MC2 1.15. The special behavior of LO** is related to the use of $\alpha_S(p_\perp^2)$ instead of $\alpha_S(Q^2)$ in the evolution. The MC-adapted distributions from CTEQ have pseudodata from full NLO calculations included in their fit. MCS is the only MC-adapted PDF that does not break the momentum sum rule, but instead has more freedom in the parameterization: renormalization and factorization scales are allowed to vary in the global fit.

Minimum-bias events are sensitive to low Q ; a Q^2 around 4 GeV^2 is a typical scale for such simulations. The up distributions for large x at $Q^2 = 4 \text{ GeV}^2$ in Fig. 1 are all similar, with slight differences for the two NLO PDFs and CT09 MC1 and MC2. The gluon distributions, on the other hand, show large differences in the small- x region: note the difference in horizontal scale. Especially MSTW LO has a much steeper rise and becomes much larger than the others. All the MRST/MSTW distributions give larger values at small x than the CTEQ ones. The MC-adapted PDFs from the respective collaboration follow each other, except for MCS which is more similar to CTEQ6L and CTEQ6L1. The two NLO PDFs stand apart from the rest, and MSTW NLO is negative in a large region. One can also note that CTEQ5L, CTEQ6L and CTEQ6L1 all freeze at $x = 10^{-6}$.

Fig. 2 shows the distributions at $Q^2 = 10^3$. Both the up and the gluon distributions show the same relative patterns as at $Q^2 = 4$. However, the differ-

ences between the PDFs are smaller, and especially the difference between the two groups are no longer as prominent, except where some PDFs freeze. At this Q^2 the CTEQ MC-adapted PDFs, in Fig. 2d, are all similar.

4 Minbias Events

Minbias events are interesting in their own right, but also because they constitute a background when studying hard interactions. They tend to have low average transverse energy, low particle multiplicity and consist largely of soft inelastic interactions. Because of the low p_\perp the interacting partons only need a small portion of the momenta of the incoming hadrons, and hence minbias events probe parton distributions in the small- x region dominated by the gluon distribution.

We examine the rapidity and multiplicity distributions from simulations with different PDFs, both at Tevatron and LHC energies. With the aid of Rivet [11] we also compare p_\perp and $\sum E_\perp$ particle spectra, as well as average p_\perp evolution with multiplicity, with data collected by the CDF experiment at Tevatron Run 2 [12].

4.1 Multiplicity and Tuning

A generator using the different PDFs needs to be retuned separately for each of them before we can make any reasonable comparisons. Specifically, the larger momentum carried by the partons in LO*, LO**, MC1 and MC2 allows a larger activity and hence a larger multiplicity than with the ordinary leading-order PDFs. Furthermore the NLO PDFs give less activity, owing to the small gluon at low x and Q^2 . We have chosen to tune PYTHIA8 so that all PDFs have the same average charged-particle multiplicity as CTEQ5L. This PDF is taken as reference because it is the default PDF in PYTHIA8 and is most commonly used in PYTHIA8 simulations. We are not making a complete tune and only intend to get a first impression of relative differences, under comparable conditions. The tuning is accomplished by tweaking the $p_{\perp 0}^{\text{Ref}}$ parameter in PYTHIA8

$$p_{\perp 0} = p_{\perp 0}^{\text{Ref}} \left(\frac{E_{\text{CM}}}{E_{\text{CM}}^{\text{Ref}}} \right)^p \quad (1)$$

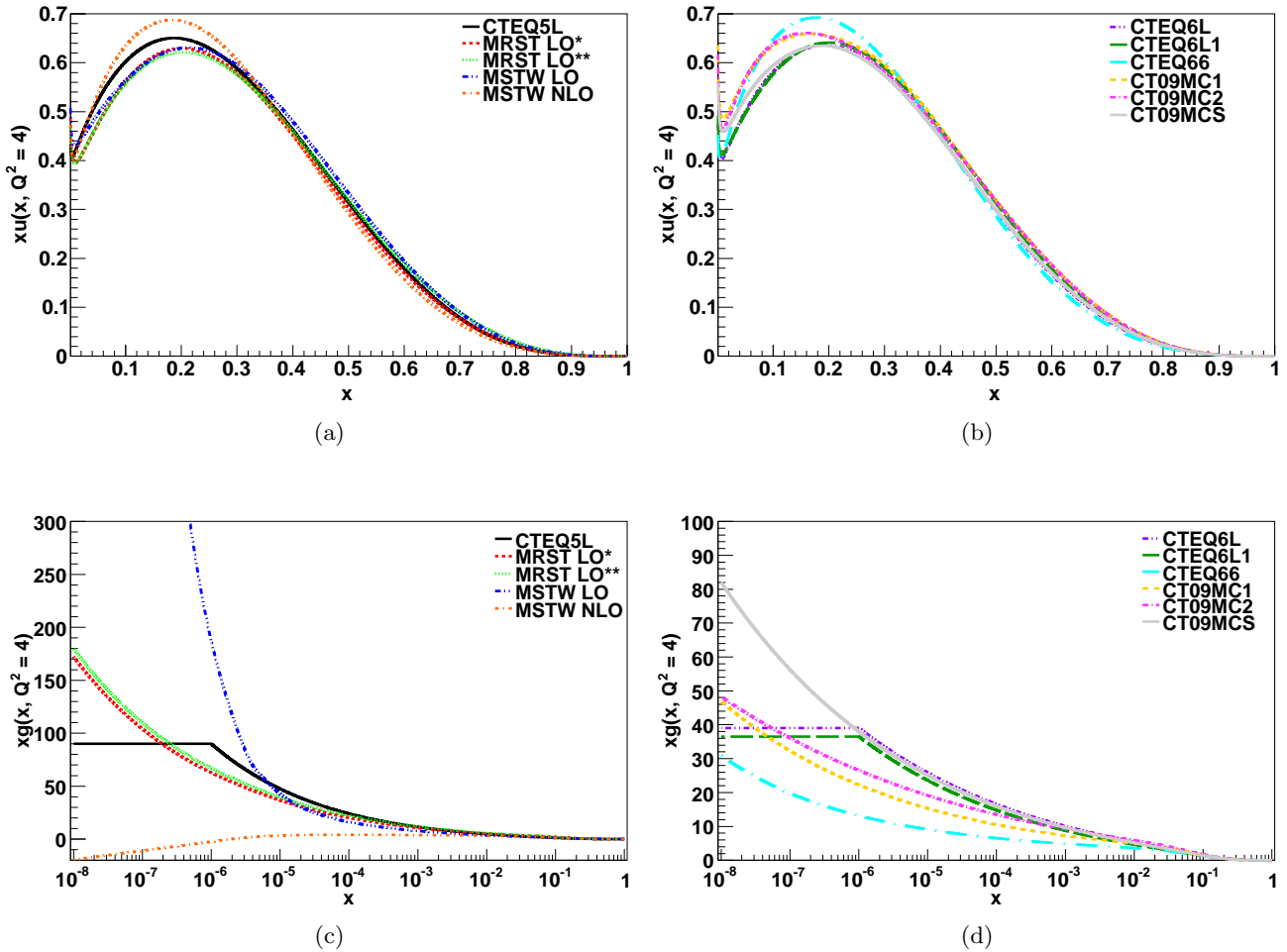


Figure 1: Up quark (a, b) and gluon (c, d) distributions at $Q^2 = 4 \text{ GeV}^2$. Note the difference in horizontal and vertical scales

where $E_{\text{CM}}^{\text{Ref}} = 1800 \text{ GeV}$ and $p = 0.24$. $p_{\perp 0}$ is used for the regularization of the divergence of the QCD cross section as $p_{\perp} \rightarrow 0$. A smaller $p_{\perp 0}$ cause the regularization to take effect at a lower p_{\perp} , increasing the charged particle multiplicity, n_{ch} . The tuning was done for the α_S value and leading-order running which is default in PYTHIA8. Results are shown in Tab. 2. The largest multiplicity before retuning is obtained with LO**, followed by MC2 and LO* which are also the PDFs with most momentum.

Further tuning could well bring some of the results closer together, but it is well known that $p_{\perp 0}^{\text{Ref}}$ is the single most crucial parameter for obtaining overall agreement with minimum-bias data at a

given energy. It is also a parameter without any constraints from theory. Other key min-bias parameters, related to the impact-parameter picture, the colour-reconnection mechanism or the beam-remnant handling, do not have as direct a coupling to the choice of PDF. The parton showers, by contrast, are better controlled by basic principles. Even if there are different shower schemes being proposed and used, within a given scheme there is no degree of freedom intended to counteract the PDF (and associated α_S) choice, in the way that $p_{\perp 0}^{\text{Ref}}$ is. The exception would be K factors for cross sections, which we will comment on later. Hadronization, finally, is fixed by the LEP data, and should not be touched.

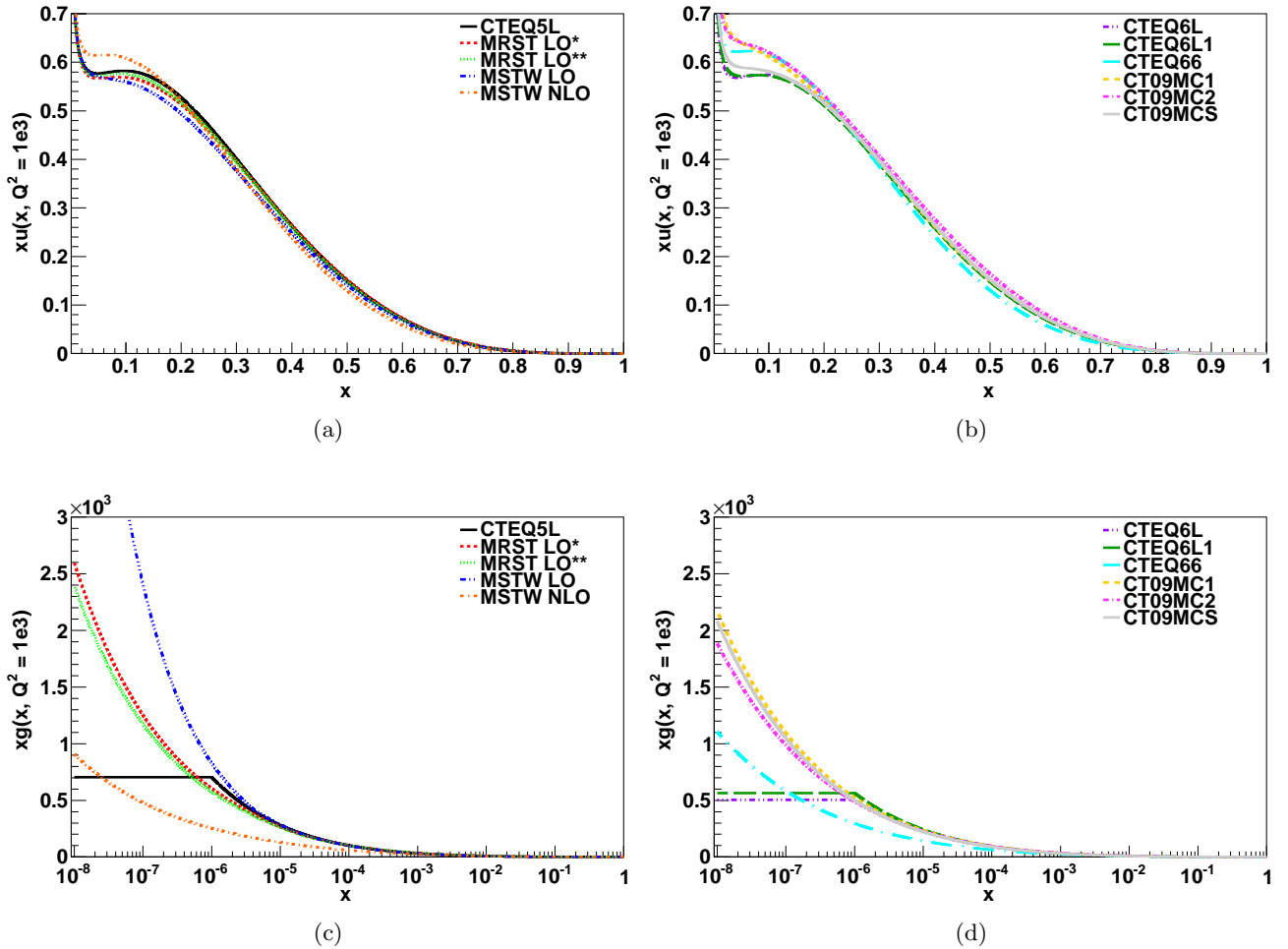


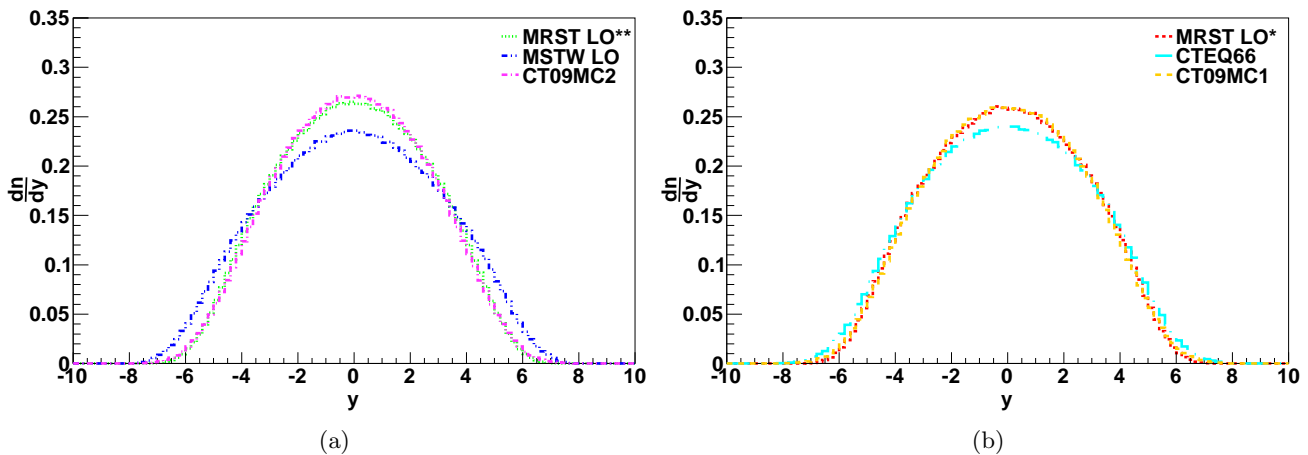
Figure 2: Up quark (a, b) and gluon (c, d) distributions at $Q^2 = 10^3 \text{ GeV}^2$. Note the difference in horizontal and vertical scales

4.2 Generator-level

In this section all simulations are for $p\bar{p}$ collisions at 1960 GeV, if not explicitly stated otherwise. So as not to crowd the plots, not all sets are shown all the time. The selection of PDFs that are shown each figure represents both the extremes and the middle way. The rapidity distributions of the outgoing particles at the parton level, when only the $2 \rightarrow 2$ sub-process is considered, are presented in Fig. 3. MSTW LO gives a broader distribution than the rest of the PDFs as an effect of the large gluon distribution at small x . The distributions with LO** and MC2 closely resemble each other, as do the distributions with LO* and MC1. This may be ex-

plained by the similarities in the violation of the momentum sum rule. The NLO PDFs give lower values in the central rapidity region. The remaining leading-order PDFs give results which are all similar to the MC-adapted ones.

Turning on the rest of the PYTHIA8 machinery, the distribution of charged particles after hadronization, shown in Fig. 4, changes in shape. There are now more particles at larger rapidities as a result of the fragmenting color field strings stretched out to the beam remnants, and most of the differences between the PDFs get blurred. Some differences still remain. MSTW LO still gives smaller multiplicity at central rapidities, and as a remnant of the wider distribution lack the inward

Figure 3: Rapidity distributions of the partons created in the $2 \rightarrow 2$ sub-process

PDF	$\langle n_{ch} \rangle$	$p_{\perp 0}^{\text{Ref}}$
CTEQ5L	54.48	2.25
MRST LO*	59.74	2.50
MRST LO**	63.52	2.63
MSTW LO	49.10	2.06
MSTW NLO	48.02	1.56
CTEQ6L	54.92	2.25
CTEQ6L1	51.71	2.13
CTEQ66	42.85	1.75
CT09MC1	53.92	2.25
CT09MC2	60.37	2.50
CT09MCS	54.87	2.25

Table 2: Average charged particle multiplicity for the different PDFs with the default value of $p_{\perp 0}^{\text{Ref}} = 2.25$ and also the $p_{\perp 0}^{\text{Ref}}$ required to tune the charge multiplicity to be equal to the value for CTEQ5L

dents that all other PDFs give at rapidities around ± 5 . The peaks for LO** and MC2 are somewhat sharper than for LO* and MC1, but the trace of the lower value with NLO PDFs at central rapidity has vanished.

The multiplicity distributions are similar for most PDFs. The two NLO distributions stand out as two extremes in different directions, MSTW NLO here gives the highest peak and the shortest tail as shown in Fig. 5. All MC-adapted PDFs, except MCS, give a peak slightly shifted to larger

multiplicities but are different in height, where the two from MRST give a larger peak value. The three normal leading-order distributions are all similar and we only show the CTEQ6L.

Increasing the energy to the level of a fully operational LHC enhances the differences seen at Tevatron energy, especially for MSTW LO and the two NLO PDFs. The multiplicity of these three evolve with energy in a different way than for the other PDFs. The rapidity distribution, shown in Fig. 6, naturally extends to larger rapidities and shows a higher central activity. MSTW LO here gives a much broader distribution. This is because as the energy increases even lower values of x come into play, so that the effect of the gluon distribution in this region has larger impact on the results. The two NLO PDFs result in flatter peaks than the MC-adapted PDFs and are similar in shape to MSTW LO. This can be explained by the smaller gluon distribution at small x . The rest of the PDFs evolve in a fashion similar to the MC-adapted PDFs shown in the figure, but with some more variation. MC1 and LO* results in a little bit larger distributions at central rapidities than MC2 and LO**.

The multiplicity distributions in Fig. 7 also show the effect of the low- x gluon distribution. MSTW LO has a much higher total multiplicity. The two NLO PDFs converge at this energy but they have smaller multiplicity than MSTW LO because of their small gluon distribution at small x . In general

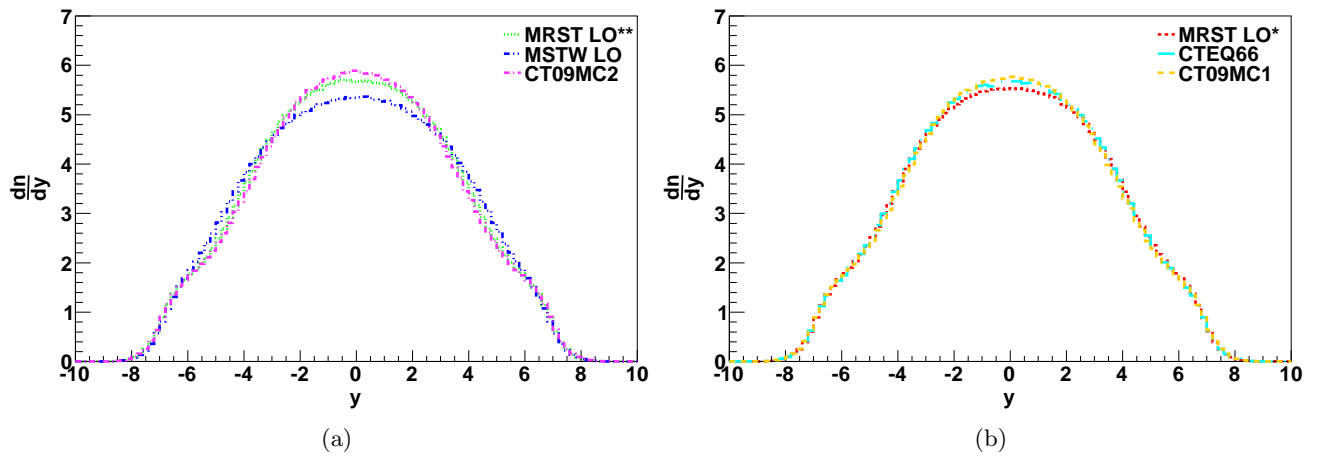


Figure 4: Rapidity distributions of charged particles after hadronization at minbias simulations with $E_{CM} = 1960$ GeV

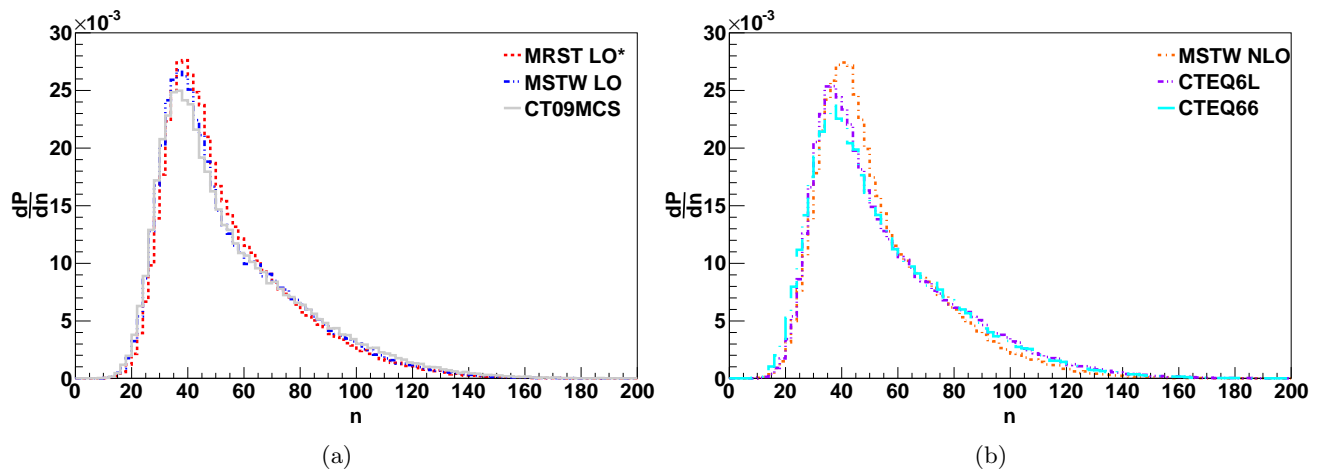


Figure 5: Charged particle multiplicity distributions

the same distributions that stand out with their rapidities also do so with their charge particle multiplicity distributions.

4.3 Comparison with CDF Run 2 data

The analyses in Rivet ensure that the comparisons to data have the same cuts and corrections as the original experiment. Therefore only the central pseudorapidity region is used and cuts in transverse momentum are implemented [12]. p_{\perp} spectra of charged particles in Fig. 8 show the same relative shape for all PDFs, which gives too large values at

the low- p_{\perp} end, then decreases compared to data and gives too small differential cross sections at the high end. The slope shows some differences depending on the choice of PDF. MC-adapted PDFs and the CTEQ6L give results that are the closest to data, while MSTW LO and NLO are further away than the rest.

The $\sum E_{\perp}$ spectrum of particles, neutral particles included, shows larger dependence on the PDFs, but the trend of disagreement of the PDFs with the data is the same as that noted for p_{\perp} . Since we have not done a complete tune, differ-

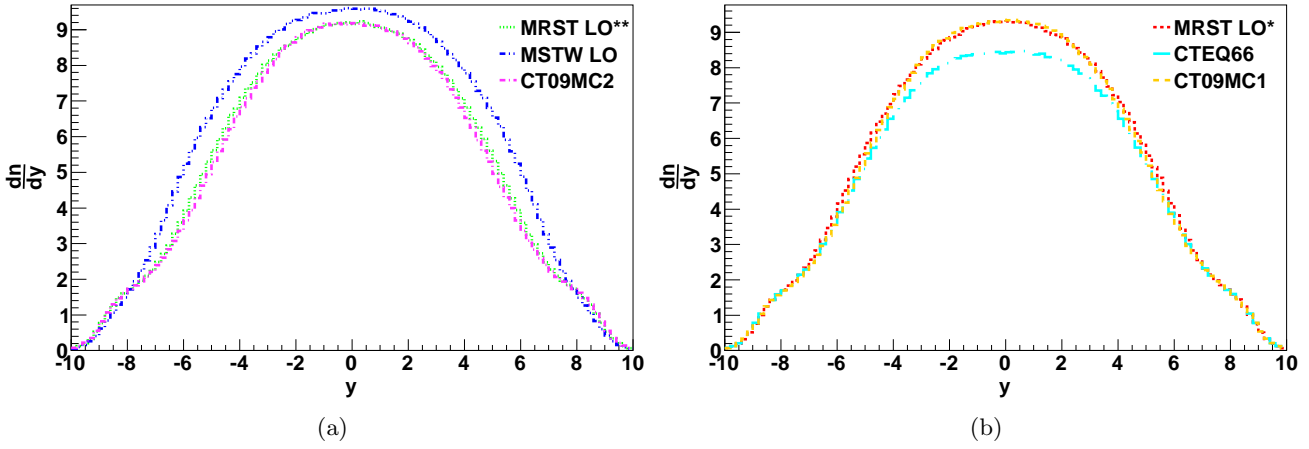


Figure 6: Rapidity distributions at LHC (pp collisions at $E_{CM} = 14$ TeV)

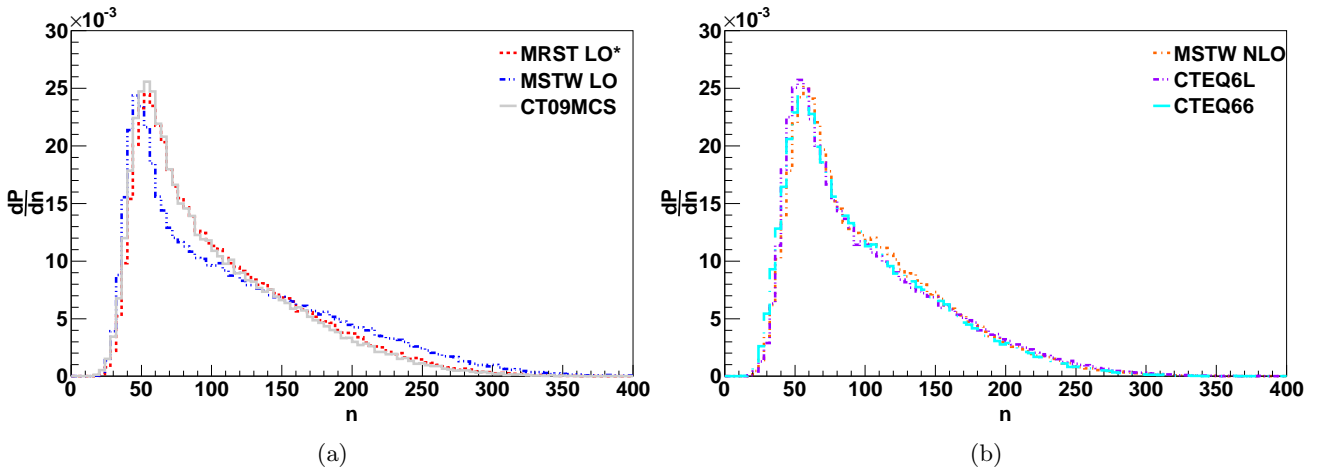


Figure 7: Charged particle multiplicity distributions at LHC

ences do indicate the importance of the PDFs. Further tuning could well bring curves closer to each other, but the $\sum E_{\perp}$ distribution is less dependent on details of the MC and therefore easier for PDF developers to consider in tunes. The MC-adapted PDFs reproduce data well while the LO and NLO PDFs give results which are further away. The exception is CTEQ6L which also gives results close to data, while MSTW LO goes down to less than half the cross section of data at the larger energy end. MSTW NLO results peak at higher energies than the rest. All PDFs give a too large value at the peak, but then decrease too fast and differ the

most from data at the high energy end.

Although different PDFs result in differences in many observables, they sometimes give more similar results. For example the evolution of the average transverse momentum with charge multiplicity reproduce the data fairly well, independent of the choice of PDF. They all give slightly too low $\langle p_{\perp} \rangle$ at low multiplicity and then increase relative to data so that they get closer as the multiplicity increases, see Fig. 10. The only PDF that gives a slightly different evolution is MSTW LO.

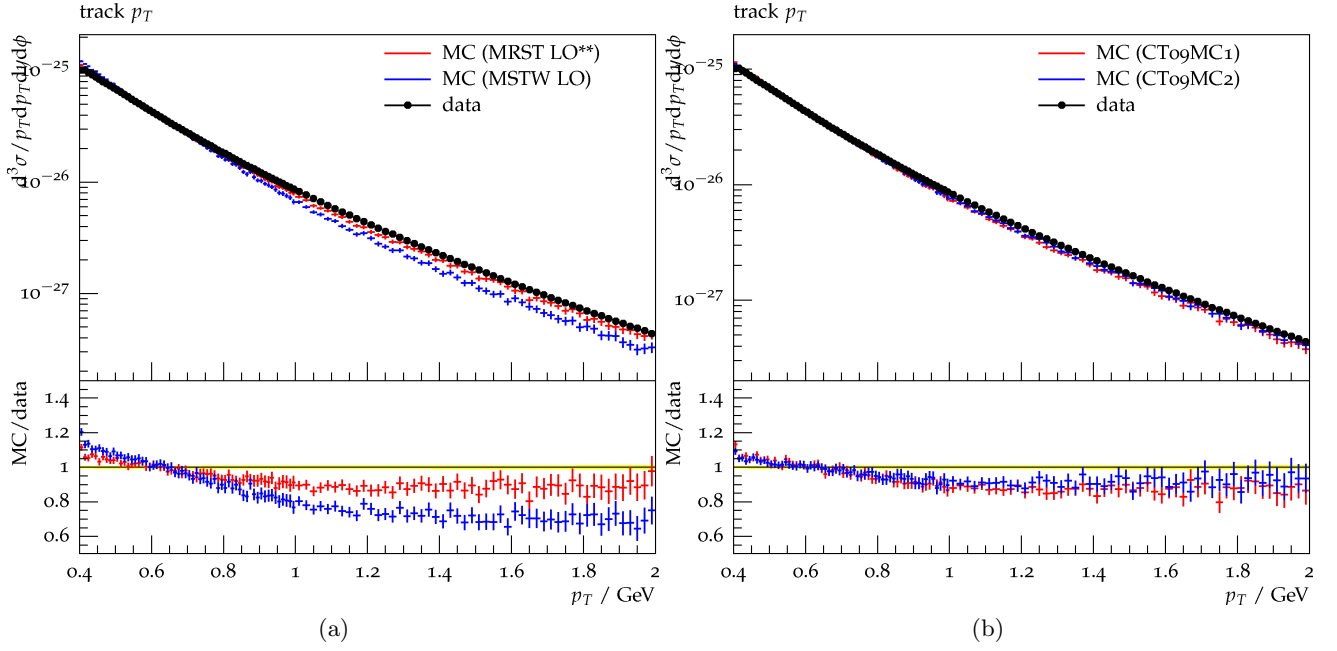


Figure 8: p_{\perp} spectra of charged particles from the CDF Run 2 experiment compared with simulations with different PDFs

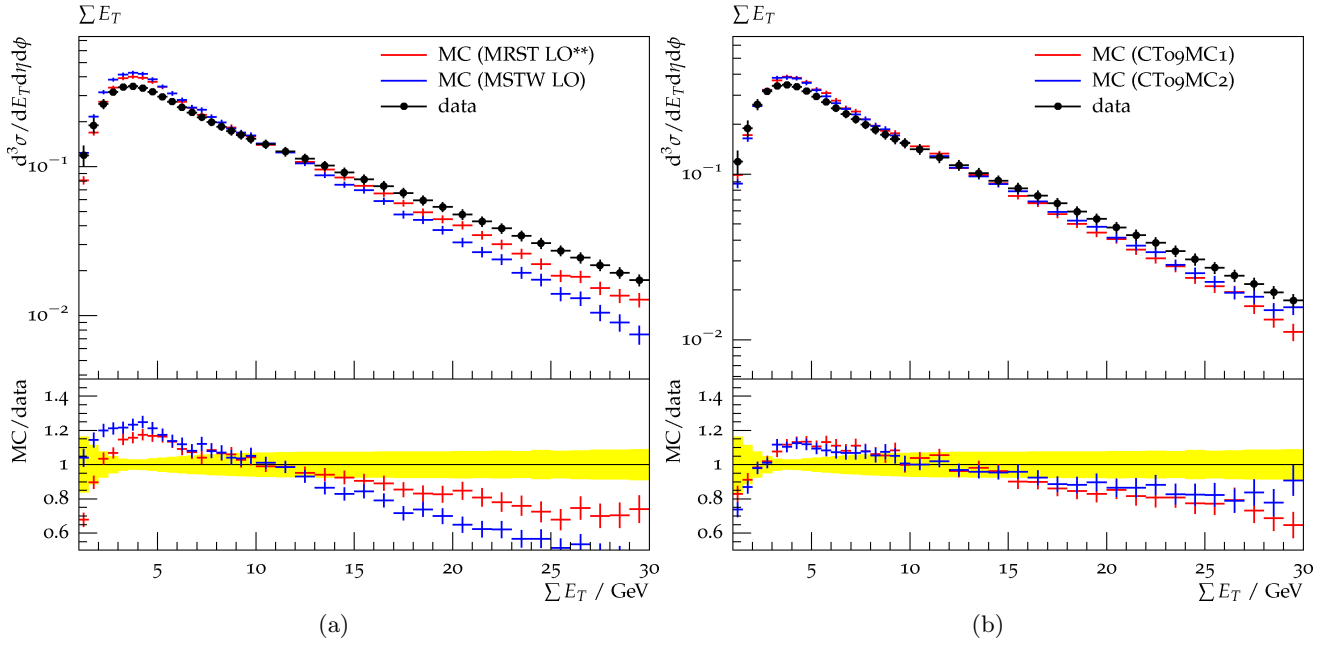


Figure 9: $\sum E_{\perp}$ spectra from the CDF Run 2 experiment compared with simulations with different PDFs

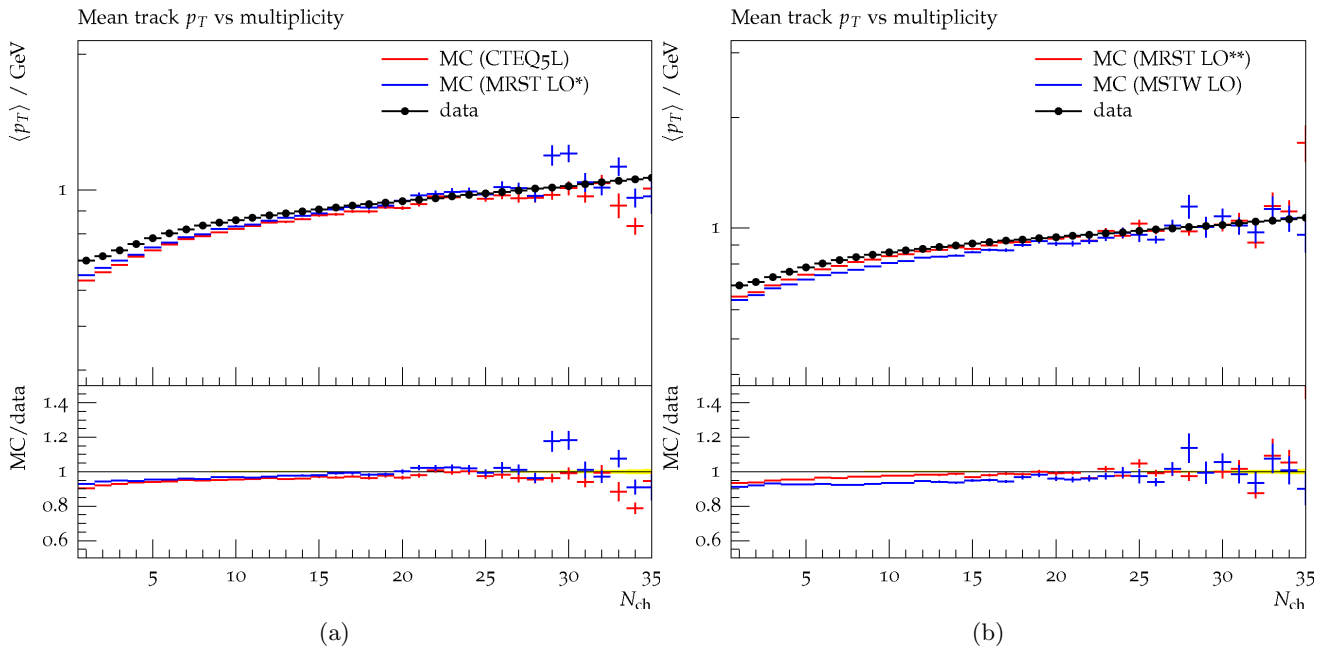


Figure 10: Evolution of the average transverse momentum, $\langle p_T \rangle$, with charge multiplicity, N_{ch} , from the CDF Run 2 experiment compared with simulations with different PDFs

5 Inclusive Jet Cross Section

We compared the inclusive jet cross sections from our MC simulations with data collected by the CDF experiment at Tevatron Run 2 [13], over five pseudorapidity intervals ranging up to $\eta \leq 2.1$. In the experimental analysis the jets are identified with the midpoint cone algorithm and also compared to results with the k_T algorithm [14]. We also examined the rapidity, multiplicity and transverse momentum distributions for the individual hadrons. Two rapidity intervals and the transverse momentum distribution have been selected to show the cross section and illustrate our findings.

The inclusive jet cross section drops rapidly with increasing p_\perp and spans over several orders of magnitude. Since this makes differences between experiments and simulations difficult to distinguish, we only show the MC/data ratio in the following figures. The results with MRST LO**, MSTW LO, CTEQ6L1, CTEQ66, CT09MC1 and CT09MC2 are shown in Fig. 11.

Generally the LO PDFs give similar results, as do the MC-adapted PDFs and the NLO PDFs are similar as well. MRST LO** starts with a much too

large cross section and the ratio quickly decreases when p_\perp rises. This behavior is the strongest for LO** at low pseudorapidity; at larger η the ratio gets smaller and flatter. All MC-adapted PDFs, except MCS, show this type of behavior. MC2 and MC1 give results with very similar shapes but the MC2 cross section is larger, and MRST LO** and LO* are related much in the same fashion. MSTW LO and CTEQ6L give cross sections which have similar behavior, and the ratio is much less dependent on p_\perp than with the MC-adapted PDFs. CTEQ6L1 gives a ratio which starts to decrease with p_\perp at larger rapidities. CT09MCS gives a too low cross section, is once again different from the other MC-adapted PDFs, and gives results which behave in a way more similar to those of the normal leading-order distributions. In the central rapidity regions the NLO PDFs actually give the cross sections closest to data with a ratio close to 1, but their ratios decrease towards 0.5 at larger η .

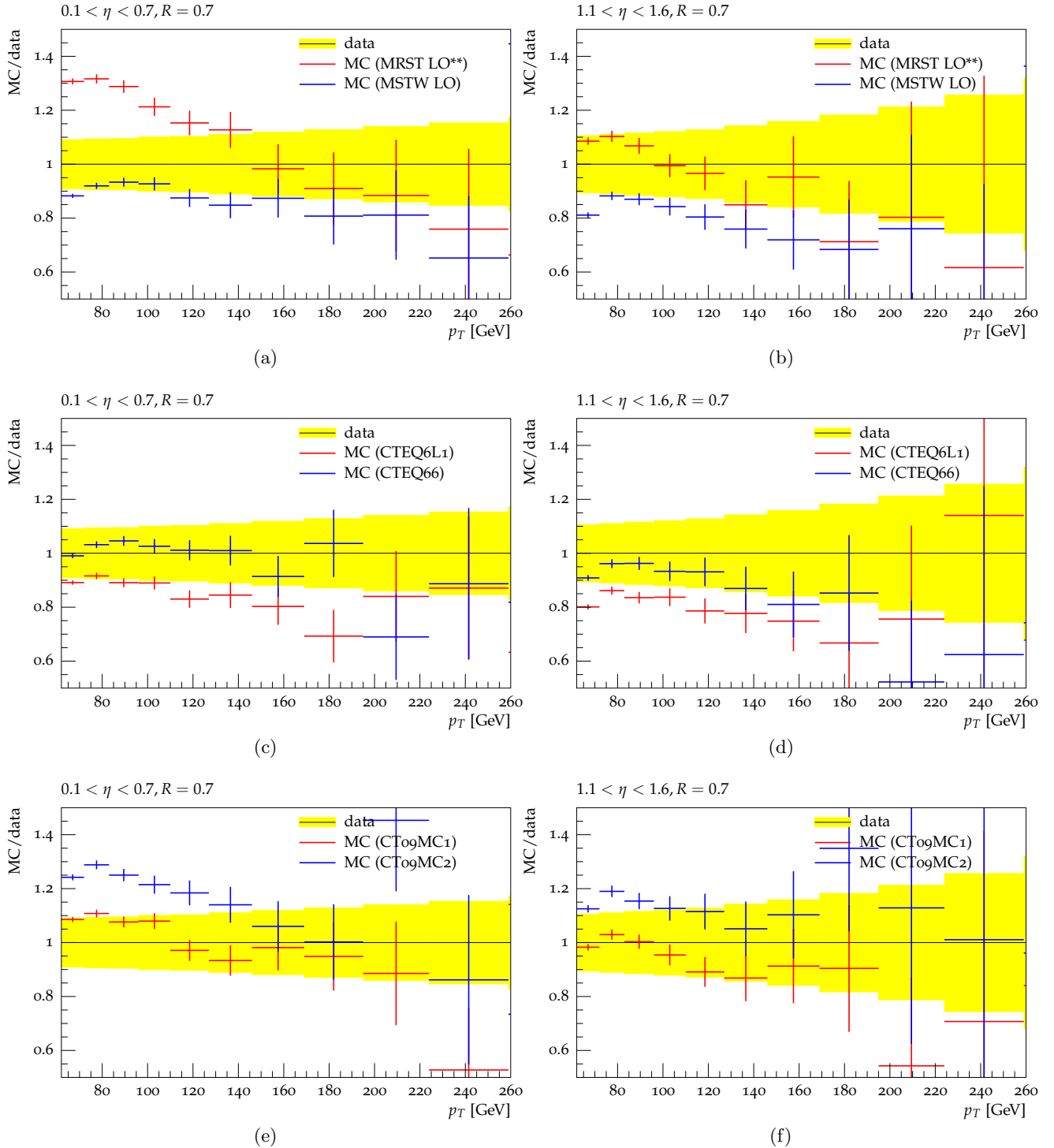


Figure 11: Ratio of the inclusive jet cross section, $MC/Data$, vs transverse momentum for two representative pseudorapidity intervals

6 Summary and Outlook

Including the very latest parton distribution functions into PYTHIA8 both caused some technical troubles and gave some surprises, especially while venturing outside the grid of the PDFs. At several occasions we were reminded that it can be risky to use NLO PDFs in LO MC generators. In addition we found that there is a need for improved numerical stability at large x , in order to keep the leading-order PDFs from going negative.

There is also a need for better understanding of parton distribution functions at small x , where the PDFs are now very different from each other. Excluding the NLO PDFs, the MRST/MSTW distributions are much larger than the ones from CTEQ, and MSTW LO goes sky high compared to all other PDFs. At larger Q^2 the differences are smaller between the two collaborations, except for the distributions that freeze their values at the end of the grid, and for MSTW LO which is still much larger than the rest. The quarks, and in particular the up distributions, at large x show smaller differences, but MSTW LO is once again larger at small x .

The large differences in the PDFs get blurred when looking at simulation results, but do nonetheless sometimes cause large variations. The MC-adapted PDFs frequently give results closer to data than the LO and NLO PDFs in their respective group. The CTEQ PDFs have distributions and give results that are more homogeneous, while the MRST/MSTW PDFs give a broader spectrum. The MC-adapted PDFs from MRST give results that show resemblance to results with the CTEQ distributions.

MSTW LO have a much larger gluon distribution at small x , which affect results of, especially, minbias simulations. The rapidity distribution is wide at the parton level ($2 \rightarrow 2$ subprocess) and at hadron level lack the inward dents at larger rapidities, which all other PDFs give. The p_{\perp} and $\sum E_{\perp}$ spectrum with this PDF have large deviations from experimental data. The inclusive jet cross section is too low and the ratio to data is fairly constant with both p_{\perp} and η . The multiplicity increases with energy at a more rapid rate than for all other PDFs.

CTEQ6L and CTEQ6L1 have a larger gluon distribution than the CTEQ MC-adapted PDFs at small x for low Q^2 , down to the freezing point, but much smaller than MSTW LO. CTEQ6L cause a rapidity distribution with a narrow peak at parton level and a slightly larger peak value at hadron level. The two distributions give similar results, but 6L is usually closer to data and hence also closer to results with the MC-adapted PDFs from CTEQ.

The two NLO PDFs, MSTW NLO and CTEQ66 are similar and also give similar results to each other for almost all observables in this study. They have the small gluon distributions characteristic of NLO PDFs, and give rapidity distributions with a low peak value at central rapidities. They are generally further away from the data in the minbias simulations, and give a slower multiplicity evolution with energy than the LO PDFs. Their inclusive jet cross section is close to data at small pseudorapidities but too low at large.

The MC-adapted PDFs which break the momentum sum rule, i.e. MRST LO*/** and CT09 MC1/2, generally give similar results to each other. They give high and narrow peaks in the rapidity distributions and are generally closer to data than the ordinary LO and NLO PDFs from their respective collaboration. The main exception is the inclusive jet cross section at low pseudorapidities and p_{\perp} , where they give too large values. Here they also give a relative decrease with p_{\perp} , a rather surprising trend which is most prominent for LO* and LO**, especially at low pseudorapidities. In the simulations of hard QCD events rapidity distributions with the MC-adapted PDFs were narrower, and their multiplicity distributions were shifted to lower multiplicity. Interesting to note is that the CT09MCS seems to have some of the features of the other MC-adapted PDFs, but in some contexts gives results more similar to ordinary leading-order PDFs.

For the leading-order PDFs a constant K -factor could improve the fit to the inclusive jet data, but for the MC-adapted PDFs the difference in shape makes it more complicated. Differences in the PDFs have a larger impact when the CM-energy of the collisions increases, and this can cause large

uncertainties in simulations at LHC energies.

Many of the differences found can be explained by the differences in the gluon distribution at small x , where we see that the middle way represented by the MC-adapted PDFs give results closer to data for many observables. It is reasonable to suspect that the results with the LO PDFs from CTEQ would resemble those of MSTW LO if extrapolated towards small x .

At this point there is no final answer as to which PDF gives the best results. In order to answer this question a much broader spectrum of observables is needed and complete tunes for the different PDFs. This study does however highlight some of the relative differences between the PDFs when they are used under comparable conditions.

During the last years there has been a renewed interest in LO tunes with focus on the applicability in MC generators. The MC-adapted PDFs resulted in some remarkable differences compared with leading-order PDF. They give results that are closer to data for many observables, although not for all. Thus there is space for further improvements. With these new PDFs a broader spectrum of tools is gained in PYTHIA8 and in examining the origin of differences and similarities between simulations and experiments. Investigations are likely to continue in relation to LHC physics.

References

- [1] A. Sherstnev and R. S. Thorne, (2008), arXiv:0807.2132v1 [hep-ph].
- [2] A. Sherstnev and R. S. Thorne, *Eur. Phys. J.* **C55**, 553 (2008), arXiv:0711.2473 [hep-ph].
- [3] H. L. Lai, J. Huston, S. Mrenna, P. Nadolsky, D. Stump, W. K. Tung and C. P. Yuan, (2009), arXiv:0910.4183 [hep-ph].
- [4] T. Sjöstrand, S. Mrenna and P. Skands, *Comput. Phys. Commun* **178** (2008) 852-867, arXiv:0170.3820 [hep-ph].
- [5] M. Glueck, E. Reya and A. Vogt, *Z.Phys.* **C67** (1995) 433.
- [6] H. L. Lai et al. [CTEQ Collaboration], *Eur. Phys. J.* **C12** (2000) 375
- [7] LHAPDF, <http://hepforge.cedar.ac.uk/lhapdf/>.
- [8] A. D. Martin, W. J. Stirling, R. S. Thorne and G. Watt, *Eur. Phys. J.* **C63** (2009) 189, arXiv:0901.0002 [hep-ph].
- [9] J. Pumplin, D. R. Stump, J. Huston, H. L. Lai, P. Nadolsky and W. K. Tung, *JHEP* **0207** (2002) 012, arXiv:hep-ph/0201195.
- [10] M. Bähr et.al., *Eur. Phys. J* **C58** (2009) 639, arXiv:0803.0883 [hep-ph]
- [11] A. Buckley et.al., *Eur. Phys. J* **C65** (2010) 331, arXiv:0907.2973 [hep-ph].
- [12] T. Aaltonen et al. [CDF Collaboration], *Phys. Rev.* **D79** (2009) 112005, arXiv:0904.1098v2 [hep-ex].
- [13] T. Aaltonen et al. [CDF Collaboration], *Phys. Rev.* **D78** (2008) 052006, arXiv:0807.2204 [hep-ex].
- [14] G. P. Salam, (2009), arXiv:0906.1833v1 [hep-ph].